

Dynamical properties of a condensate in a moving random potential

Ardavan Alamir^{1,a}, Pablo Capuzzi^{2,3}, and Patrizia Vignolo¹

¹ Université de Nice – Sophia Antipolis, Institut non Linéaire de Nice, CNRS, 1361 route des Lucioles, 06560 Valbonne, France

² Departamento de Física, Facultad de Ciencias Exactas y Naturales, Universidad de Buenos Aires, 1428 Buenos Aires, Argentina

³ Instituto de Física de Buenos Aires – CONICET, Argentina

Received 7 September 2012 / Received in final form 15 January 2013

Published online 11 March 2013

Abstract. We study the dynamics of an inhomogeneous Bose-Einstein condensate subject to a one-dimensional harmonic trap and a moving random potential of finite extent. Above the critical velocity, a part of a condensate glues to the moving random potential with a consequent displacement of the condensate center-of-mass along the harmonic trap. We show that the center-of-mass turning point provides a direct measure of the average drag force acting on the condensate.

1 Introduction

The study of complex systems, such as many-body systems characterized by inter-particle interactions and disorder is one of the outstanding challenges of physics. In the presence of significant interactions, the disorder can induce exotic phases on lattice systems [1], and shift the onset of superfluidity in continuum systems at lower [2,3] or even larger [2] critical temperatures. In the superfluid regime, the presence of a random potential does not perturb the low-energy dynamics of the system itself. Indeed, below a critical velocity v_{cr} that depends on the gas density and on the disorder strength [4–7], the superfluid does not scatter against the potential defects by its superfluid nature. On the contrary, at velocities greater than v_{cr} , superfluidity breaks down and the interference of the scattered waves may deeply modify the fluid transport [8–10] unto the Anderson localization regime [11,12]. In a confined system where the density is inhomogeneous, superfluidity breaks down beforehand in the low density regions and one may observe the inhibition of the expansion [13], the dipolar mode damping [14], and the localization of a piece of the system [15]. Differently and in complementarity with [15], in this paper we focus on the dynamical evolution of the localized fraction of a cigar-shaped Bose-Einstein condensate (BEC) subject to a moving random potential. We analyze the density and center-of-mass time-evolution of the system, comparing two types of disorder potentials characterized by different correlation functions. The paper is organized as following. In Sect. 2 we describe the

^a e-mail: ardavan.alamir@inln.cnrs.fr

model of the systems and, in Sect. 3, we discuss our numerical results. Finally, some concluding remarks are given in Sect. 4.

2 The model

We focus on a system of $N = 10^5$ Bose-Einstein condensed 87-Rubidium atoms of mass m subject to a static cigar-shaped harmonic trap and a time-dependent random potential:

$$U(\mathbf{r}, t) = \frac{1}{2}m\omega_{\perp}^2(x^2 + y^2) + \frac{1}{2}m\omega_z^2z^2 + V(z, t) \quad (1)$$

with $\omega_{\perp} = 2\pi \times 500$ Hz and $\omega_z = 2\pi \times 7$ Hz the trapping frequencies in the perpendicular and longitudinal directions, respectively. The last time-dependent term in (1) corresponds to a random potential that is fixed in the moving frame $z' = z - vt$, $\mathbf{v} = v\hat{e}_z$ being the drift velocity. This potential is modeled by the sum of N_{dis} Gaussian functions of height V_{dis} and width w distributed at positions $z_i = j_i d$, where j_i is a random integer number and d fixes the minimal distance between the peaks. This type of disorder, known as Edwards model [16], could be realized by pinning some heavy impurities in the minima of a periodic potential as proposed previously [17, 18].

Under cigar-shaped trap geometry, the full 3D equation of motion for the BEC wavefunction $\psi(\mathbf{r}, t)$ can be reduced to the effective 1D time-dependent nonpolynomial nonlinear Schrödinger equation (NPSE) [19]

$$i\hbar \frac{\partial}{\partial t} f = \left[-\frac{\hbar^2}{2m} \frac{\partial^2}{\partial z^2} + \frac{1}{2}m\omega_z^2 z^2 + V(z, t) + \hbar\omega_{\perp} \frac{1 + 3a_s N|f|^2}{\sqrt{1 + 2a_s N|f|^2}} \right] f. \quad (2)$$

a_s being the s -wave scattering length. To obtain Eq. (2) we set

$$\psi(\mathbf{r}, t) = f(z, t)\phi(\mathbf{r}, t) = f(z, t) \frac{e^{-(x^2+y^2)/2\sigma^2(z,t)}}{\sqrt{\pi}\sigma(z, t)} \quad (3)$$

where the transverse part $\phi(\mathbf{r}, t)$ is modeled by a Gaussian function with variance $\sigma(z, t)$. Within the assumption that this variance varies slowly as functions of z and t , $\sigma(z, t)$ is given by

$$\sigma^2(z, t) = \ell_0^2 \sqrt{1 + 2a_s N|f(z, t)|^2}, \quad (4)$$

where $\ell_0 = \sqrt{\hbar/(m\omega_{\perp})}$ is the oscillator length in the transverse direction. The 3D density profile is then

$$\rho(\mathbf{r}) = \tilde{\rho}(z) \frac{e^{-(x^2+y^2)/\sigma^2}}{\pi\sigma^2}, \quad (5)$$

with $\tilde{\rho}(z) = |f|^2$ the integrated 1D density.

3 Numerical results

We study and compare the BEC dynamics in the presence of two types of moving Edwards disorders: (i) an Anderson-like distribution (AM), where the j_i 's are randomly distributed; (ii) a Random Dimer Model (RDM) distribution where peaks are dimerized and the dimers are randomly distributed [20]. Hereafter we consider a disorder potential characterized by an amplitude $V_{\text{dis}} = 0.02E_r$, where the recoil energy $E_r = \hbar^2/(2m\lambda^2)$ is defined with respect to the wavelength $\lambda = 780$ nm, characterizing the D2 hyperfine Rubidium transition. The dimer peak-to-peak distance ℓ , as well as the minimum distance d between single defects are set equal to λ ; the width of a single bump w is fixed at 140 nm.

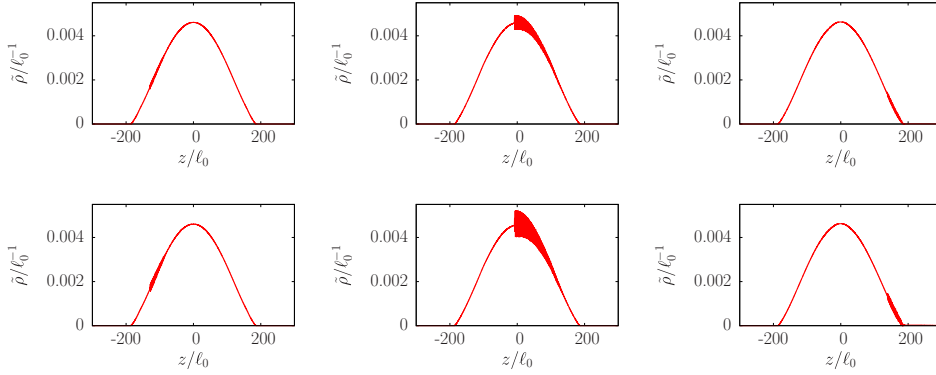


Fig. 1. Integrated density profiles $\tilde{\rho}$ as functions of the position for the moving single defect (top row) and moving single dimer (bottom row) at a velocity $v = 1.4c$. The left, middle and right columns correspond to $t = 0.75/\omega_z$, $1.5/\omega_z$ and $2.4/\omega_z$, respectively.

3.1 Density profiles

We first study the effect of a single defect for the two models (i) and (ii) on the dynamical evolution of the BEC density profile. Both the single bump and the single dimer drag some atoms as they move through the fixed parabolic trap. This is illustrated in Fig. 1 in the spatial profile of the density as both objects move with the same velocity $v = 1.4c$, $c = \sqrt{\mu/(2m)}$ being the BEC sound velocity in a cigar-shaped geometry [21] at the trap center. At this drift velocity, the dimer perturbs the BEC more than twice a single defect in its trajectory through the density profile. In fact, we found that the center of mass is shifted by a factor of about 3 with respect to the single defect. The scattering properties of a single dimer depend on the drift velocity non-monotonically [15], so that in some energy regions, as in this case, the dimer may drag the BEC more efficiently than two uncorrelated single defects or may help delocalization [20].

In the presence of several defects, the dynamical evolution changes qualitatively and the number of atoms dragged by the moving potential increases as well. We focus on the case with a density of peaks $n_{\text{dis}} \simeq 0.12\lambda^{-1} \simeq 0.16 \text{ peaks}/\mu\text{m}$ (the same for the AM and the RDM), moving through the BEC with drift velocities $v = 1.2c$, $1.5c$ and $1.8c$. Figure 2 displays the density profiles at a time corresponding to a displacement of the moving potential of about $96\mu\text{m} \simeq 200\ell_0$. We observe that the perturbations on the parabolic potential are more irregular than for the single defect case, and that depending on the value of v , more atoms are dragged either by the AM or the RDM potentials. For the parameters here considered we find that for the low velocity case, the AM potential drags more atoms than the RDM potential, whereas we increase v the RDM becomes more efficient to localize and, hence, drag more atoms along the moving potential.

The dependence of the fraction of dragged atoms N_d/N on the type of disorder and on its velocity can be more simply read from the center-of-mass displacement z_{cm} of the BEC as already discussed in [15]. The underlying idea is that N_d/N equals the ratio between z_{cm} and the disorder displacement vt . As illustrated in Fig. 3 this quantity depends on time showing that the atoms need some time to be affected by the moving potential. This delay stems from the time needed to scatter from one bump to another and to establish the interference of the scattered matter waves. The importance of the interference effects in the dynamics is supported by the dependence of N_d/N on the correlation function of the disorder potential. In addition, we observe in Fig. 3 that the curves in the AM and RDM cases do not intersect showing that for

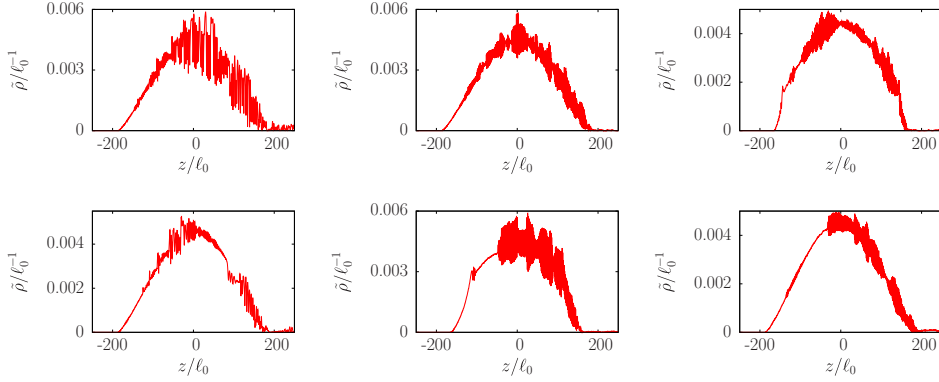


Fig. 2. Integrated density profiles $\tilde{\rho}$ for the AM (top row) and RDM (bottom row) random potentials. The left, middle and right column correspond to drift velocities $v/c = 1.2, 1.5, 1.8$ respectively. The densities are displayed for times corresponding to the same displacement of the moving potential.

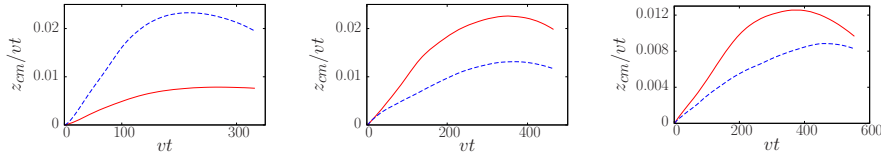


Fig. 3. Center-of-mass positions as functions of the displacement vt of the moving potential. Blue dashed and red continuous lines correspond to AM and RDM, respectively. Panels from left to right correspond to $v = 1.2 c$, $v = 1.5 c$, $v = 1.8 c$.

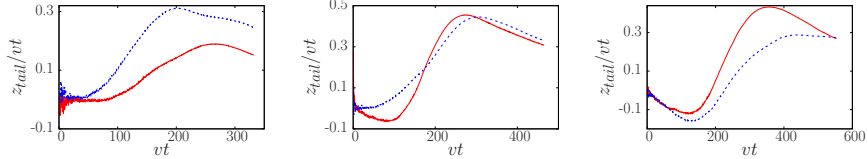


Fig. 4. The same as for Fig. 3 but for the barycenter z_{tail} of the forward tail populated by 1% of the atoms.

all times one of the disorder potentials drags more effectively the atoms for a given velocity, irrespectively of the initial delay.

The atoms dragged by the moving potential belong mainly to the tails of the density profiles. This is shown in Fig. 4 where we have plot the time evolution of the barycenter z_{tail} of the forward tail populated by 1% of the atoms. This inhomogeneous distribution of the dragged atoms is due to the density inhomogeneity imposed by the harmonic potential since at low densities v_{cr} is lower and thus the atomic scattering becomes more efficient.

The maximum displacement z_f of the center of mass is determined by the competition between the drag force

$$F_{\text{dis}} = - \int_{-\infty}^{+\infty} dz |f(z, t)|^2 \frac{\partial V}{\partial z} \quad (6)$$

induced by the moving random potential and the force exerted by the harmonic confinement. The dynamics of F_{dis} is very complex and cannot be evaluated in an

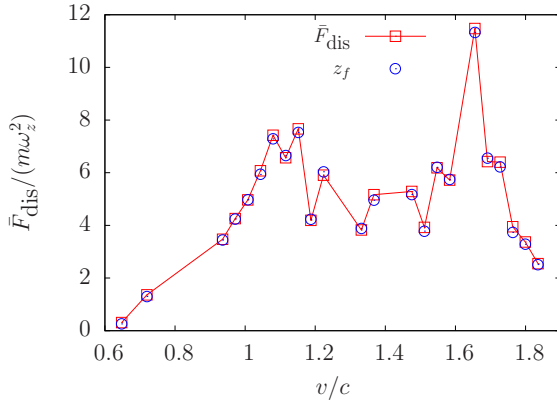


Fig. 5. Average drag force \bar{F}_{dis} compared with the turning point z_f (in units of ℓ_0) for the AM disorder potential as functions of the drift velocity v .

experiment. However its average value $\bar{F}_{\text{dis}} = \int_0^{z_f} F_{\text{dis}} dz_{\text{cm}} / z_f$ provides information about the localization efficiency of a given random potential and can be straightforwardly evaluated by the turning point z_f as shown in [15]. Indeed we found that $z_f = 2\bar{F}_{\text{dis}} / (\bar{m}\omega_z^2)$. This is numerically confirmed by the comparison of z_f with \bar{F}_{dis} obtained by averaging the value of the drag force (6) during the simulation as shown in Fig. 5 for the AM disorder and the whole range of drift velocities analyzed.

4 Concluding remarks

In this paper we investigated the dynamical evolution of a cigar-shaped BEC subject to a moving random potential. A fraction of the atoms belonging to the low density regions of the BEC glue to the random potentials. This fraction depends on the velocity and type of correlation of the disorder potential indicating that the localization occurs by interference effects.

This work was supported by CNRS PICS grant No. 05922. P. C. acknowledges support from ANPCyT and CONICET, Argentina through grants PICT 2008-0682 and PIP 0546, respectively.

References

1. M.P.A. Fisher, P.B. Weichman, G. Grinstein, D.S. Fisher, Phys. Rev. B **40**, 546 (1989)
2. Pilati, S. Giorgini, N. Prokofev, Phys. Rev. Lett. **102**, 150402 (2009)
3. B. Allard, T. Plisson, M. Holzmann, G. Salomon, A. Aspect, P. Bouyer, T. Bourdel, Phys. Rev. A **85**, 033602 (2012)
4. R. Onofrio, C. Raman, J.M. Vogels, J.R. Abo-Shaeer, A. P. Chikkatur, W. Ketterle, Phys. Rev. Lett. **85**, 2228 (2000)
5. G.E. Astrakharchik, L.P. Pitaevskii, Phys. Rev. A **70**, 013608 (2004)
6. S. Ianeselli, C. Menotti, A. Smerzi, J. Phys. B **39**, S135 (2006)
7. R. Citro, A. Minguzzi, F.W.J. Hekking, Phys. Rev. B **79**, 172505 (2009)
8. T. Paul, P. Schlagheck, P. Leboeuf, N. Pavloff, Phys. Rev. Lett. **98**, 210602 (2007)
9. T. Paul, M. Albert, P. Schlagheck, P. Leboeuf, N. Pavloff, Phys. Rev. A **80**, R2664 (2009)
10. M. Albert, T. Paul, N. Pavloff, P. Leboeuf, Phys. Rev. A **82**, 011602 (2010)

11. P.W. Anderson, Phys. Rev. **109**, 1492 (1958)
12. P.W. Anderson, Philosophical Magazine Part B **52**, 505 (1985)
13. C. Fort, L. Fallani, V. Guarrera, J.E. Lye, M. Modugno, D.S. Wiersma, M. Inguscio, Phys. Rev. Lett. **95**, 170410 (2005)
14. M. Albert, T. Paul, N. Pavloff, P. Leboeuf, Phys. Rev. Lett. **100**, 250405 (2008)
15. A. Alamir, P. Capuzzi, P. Vignolo, Phys. Rev. A **86**, 063637 (2012)
16. E. Akkermans, G. Montambaux, *Mesoscopic physics of electrons and photons* (Cambridge University Press, New York, 2007)
17. P. Vignolo, Z. Akdeniz, M.P. Tosi, J. Phys. B: At. Mol. and Opt. Phys. **36**, 4535 (2003)
18. U. Gavish, Y. Castin, Phys. Rev. Lett. **95**, 020401 (2005)
19. L. Salasnich, A. Parola, L. Reatto, Phys. Rev. A **65**, 043614 (2002)
20. D.H. Dunlap, H-L. Wu, P.W. Phillips, Phys. Rev. Lett. **65**, 88 (1990)
21. E. Zaremba, Phys. Rev. A **57**, 518 (1998)